http://ansinet.com/itj

ITJ

ISSN 1812-5638

INFORMATION TECHNOLOGY JOURNAL

ANSInet
Asian Network for Scientific Information
308 Lasani Town, Sargodha Road, Faisalabad - Pakistan

Information Technology Journal 6 (8): 1171-1180, 2007
ISSN 1812-5638

A Study into the Merit of the DCT Based NGVF Active Contours in Comparison with DCT Based GVF Active Contours

[1]A. Prabhu Britto and [2]G. Ravindran
[1]Center for Medical Electronics, Department of Electronics and Communication Engineering,
[2]Faculty of Information and Communication Engineering, Anna University, Chennai, India

Abstract: This research studies the Discrete Cosine Transform Based Gradient Vector Flow in Normal Direction (DCT based NGVF) Active Contours in comparison with the Discrete Cosine Transform Based Gradient Vector Flow (DCT based GVF) Active Contours. Extensive research has been done on DCT based GVF Active Contours and the strengths of DCT based GVF Active Contours have been established. NGVF, the recent improvement to the GVF Active Contour has faster convergence speed towards the concavity and bigger time step. It also has the capability to enter into long, thin indention and provide a good contour. The DCT based NGVF Active Contours has the combined strengths of the NGVF Active Contours and the DCT based GVF Active Contour formulation. This research experimentally studies the merit of the DCT based NGVF Active Contours in comparison with the DCT based GVF Active Contours. The experimental inferences shed more light on the comparative merits of DCT based NGVF Active Contours.

Key words: Gradient Vector Flow, Discrete Cosine Transform Based Gradient Vector Flow, Discrete Cosine Transform Based Gradient Vector Flow in normal direction

INTRODUCTION

This research studies the Discrete Cosine Transform Based Gradient Vector Flow in Normal Direction (DCT based NGVF) Active Contours in comparison with the Discrete Cosine Transform Based Gradient Vector Flow (DCT based GVF) Active Contours. DCT based NGVF Active Contours have been proposed by Britto and Ravindran (2007c). The DCT based NGVF Active Contours has its foundation derived from NGVF Active Contours (Jifeng *et al*., 2007) and extensive research carried out in the area of image segmentation using GVF Active Contours (Britto and Ravindran, 2005a, b; 2006a-e; 2007a, b).

Active Contours are used extensively in computer vision and image processing applications, particularly to locate object boundaries. The main advantage of Active Contours is the ability to generate closed parametric curves from images. Problems associated with initialization and poor convergence to concave boundaries, however, have limited their utility.

To overcome these difficulties in initialization and poor convergence to object boundaries, an external force model was suggested that used a convex combination of the usual external force and a new force derived from an estimate of the local curvature of the object boundary. This force simultaneously pulled the snake toward the boundary and into the concave region (Prince and Xu, 1996). This was later improved by Xu and Prince to form the Gradient Vector Flow (GVF) field.

The resulting formulation produces external force fields that had both irrotational and solenoidal components (Xu and Prince, 1998), which had a large capture range overcoming the difficulty associated with initialization of Active Contours and it was also able to provide good convergence to concave boundaries. Tang and Acton (2004) have given an improved form of the GVF field, called the Discrete Cosine Transform (DCT) based GVF.

Extensive experimentation and analysis on the chromosome spread image segmentation performance of DCT based GVF Active Contours has been performed and it is established that the DCT based GVF Active Contours are an efficient segmentation technique for chromosome images (Britto and Ravindran, 2005a, b; 2006a-e; 2007a, b).

An improvement for the GVF Active Contours called NGVF (GVF in the Normal direction) has been proposed (Jifeng *et al*., 2007). The NGVF has faster convergence

Corresponding Author: A. Prabhu Britto, Center for Medical Electronics,
Department of Electronics and Communication Engineering,
Anna University, Chennai 600025, India

speed towards the concavity and bigger time step. It also has the capability to enter into long, thin indention and provide a good contour. The DCT based NGVF Active Contours had been proposed (Britto and Ravindran, 2007c) based on the strengths of GVF Active Contours and NGVF Active Contours.

ACTIVE CONTOUR MODELS

Active Contours also called as snakes or deformable curves, first proposed by Kass *et al.* (1987) are energy minimizing contours that apply information about the boundaries as part of an optimization procedure. They are generally initialized by automatic or manual process around the object of interest. The contour then deforms itself iteratively from its initial position in conformity with the nearest dominant edge feature, by minimizing the energy composed of the internal and external forces, converging to the boundary of the object of interest.

The internal forces computed from within the Active Contour enforce smoothness of the curve and external forces that are derived from the image help to drive the curve toward the desired features of interest during the course of the iterative process. The energy minimization process can be viewed as a dynamic problem where the Active Contour Model is governed by the laws of elasticity and lagrangian dynamics (Rueckert, 1997) and the model evolves until equilibrium of all forces is reached, which is equivalent to a minimum of the energy function. The energy function is thus minimized, making the model active.

FORMULATION OF ACTIVE CONTOUR MODELS

An Active Contour Model can be represented by a curve c, as a function of its arc length τ:

$$c(\tau) = \begin{pmatrix} x(\tau) \\ y(\tau) \end{pmatrix} \quad (1)$$

with $\tau = [0...1]$. To define a closed curve, c(0) is set to equal c(1). A discrete model can be expressed as an ordered set of n vertices as $v_i = (x_i,y_i)^T$ with $v=(v_1,\ldots,v_n)$. The large number of vertices required to achieve any predetermined accuracy could lead to high computational complexity and numerical instability (Rueckert, 1997).

Mathematically, an Active Contour Model can be defined in discrete form as a curve x(s) = [x(s), y(s)], $s\varepsilon[0,1]$ that moves through the spatial domain of an image to minimize the energy functional:

$$E = \int_0^1 \frac{1}{2}(\alpha|x'(s)^2 + \beta|x''(s)^2) + E_{ext}(x(s))ds \quad (2)$$

Where, α and β are weighting parameters that control the Active Contour's tension and rigidity, respectively (Xu and Prince, 1997). The first order derivative discourages stretching while the second order derivative discourages bending. The weighting parameters of tension and rigidity govern the effect of the derivatives on the snake. The external energy function E_{ext} is derived from the image so that it takes on smaller values at the features of interest such as boundaries and guides the Active Contour towards the boundaries. The external energy is defined by

$$E_{ext} = \kappa|G_\sigma(x,y) * I(x,y)| \quad (3)$$

Where, $G_\sigma(x,y)$ is a two-dimensional Gaussian function with standard deviation σ, I(x,y) represents the image and κ is the external force weight. This external energy is specified for a line drawing (black on white) and positive κ is used. A motivation for applying some Gaussian filtering to the underlying image is to reduce noise.

An Active Contour that minimizes E must satisfy the Euler Equation

$$\alpha x''(s) - \beta''''(s) - \nabla E_{ext} = 0 \quad (4)$$

Where, $F_{int} = \alpha x''(s) - \beta x''''(s)$ and $F_{ext} = -\nabla E_{ext}$ comprise the components of a force balance equation such that

$$F_{int} + F_{ext} = 0 \quad (5)$$

The internal force F_{int} discourages stretching and bending while the external potential force F_{ext} drives the active contour towards the desired image boundary. Eq. 4 is solved by making the Active Contour dynamic by treating x as a function of time t as well as s. Then the partial derivative of x with respect to t is then set equal to the left hand side of Eq. 4 as follows:

$$x_t(s,t) = \alpha x''(s,t) - \beta x''''(s,d) - \nabla E_{ext} \quad (6)$$

A solution to Eq. 6 can be obtained by discretizing the equation and solving the discrete system iteratively (Kass *et al.*, 1987). When the solution x(s,t) stabilizes, the term $x_t(s,t)$ vanishes and a solution of Eq. 4 is achieved. Traditional Active Contour Models suffer from a few drawbacks. Boundary concavities leave the contour split

across the boundary. Capture range is also limited. Hence a new external force was developed (Prince and Xu, 1996).

Three guiding principles led to the development of the new external force.

- The first aim was the ability to add the new force to the existing force. Since the existing force was the gradient of a scalar function (the energy E_{ext}), it was an irrotational (curl-free field). According to the Helmholtz theorem, the other fundamental field component was a solenoidal (divergence-free) field. Therefore, the new field was chosen to be solenoidal.
- The second aim was that the new field should not disturb the equilibrium contours of the external energy in the absence of internal forces. Therefore, the new field should be zero whenever the field $-\nabla E_{ext}$ is zero.
- The third aim wanted the field to point toward the apex of concave boundary regions, a feature defined by the object boundary curvature. Therefore, the new field was made to use a measure of boundary curvature in its definition (Prince and Xu, 1996). This was later improved by Xu and Prince to form the GVF field. Xu and Prince (1997) presented a new external force, called GVF, which was computed as a diffusion of the Gradient Vectors of a gray-level or binary edge map derived from the image. The resultant field had a large capture range and forces the Active Contours into concave regions (Xu and Prince, 1998, 2000).

The overall approach was to define a new non-irrotational external force field, called as the GVF field. The earlier idea of constructing a separate solenoidal field from an image and adding it to a standard irrotational field was improved and a more natural approach was designed in which the external force field is designed to have the desired properties of both large capture range and presence of forces that point into boundary concavities. The resulting formulation produces external force fields that had both irrotational and solenoidal components (Xu and Prince, 1998).

GRADIENT VECTOR FLOW (GVF) ACTIVE CONTOURS

Gradient Vector Flow (GVF) Active Contours use Gradient Vector Flow fields obtained by solving a vector diffusion equation that diffuses the Gradient Vectors of a gray-level edge map computed from the image. The GVF Active Contour Model cannot be written as the negative gradient of a potential function. Hence it is directly specified from a dynamic force equation, instead of the standard energy minimization network. The external forces arising out of GVF fields are non-conservative forces as they cannot be written as gradients of scalar potential functions. The usage of non-conservative forces as external forces show improved performance of GVF field Active Contours compared to traditional energy minimizing Active Contours (Xu and Prince, 1998, 2000). The GVF field points towards the object boundary when very near to the boundary, but varies smoothly over homogeneous image regions extending to the image border. Hence the GVF field can capture an Active Contour from long range from either side of the object boundary and can force it into the object boundary. The GVF Active Contour Model thus has a large capture range and is insensitive to the initialization of the contour. Hence the contour initialization is flexible.

The Gradient Vectors are normal to the boundary surface but by combining Laplacian and Gradient the result is not the normal vectors to the boundary surface. As a result of this, the GVF field yields vectors that point into boundary concavities so that the Active Contour is driven through the concavities. Information regarding whether the initial contour should expand or contract need not be given to the GVF Active Contour Model. The GVF is very useful when there are boundary gaps, because it preserves the perceptual edge property of Active Contours (Kass *et al*., 1987; Xu and Prince, 1998). The GVF field is defined as the equilibrium solution to the following vector diffusion equation (Xu and Prince 2000),

$$u_t = g(|\nabla f|)\nabla^2 u - h(|\nabla f|)(u - \nabla f) \quad (7a)$$

$$u(x,0) = \nabla f(x) \quad (7b)$$

Where:

u_t = Partial derivative of u(x,t) with respect to t

∇^2 = Laplacian operator (applied to each spatial component of u separately)

f = An edge map that has a higher value at the desired object boundary.

The functions in g and h control the amount of diffusion in GVF. In Eq. 7, $g(|\nabla f|)\nabla^2 u$ produces a smoothly varying vector field and hence called as the smoothing term, while $h(|\nabla f|)(u-\nabla f)$ encourages the vector field u to be close to ∇f computed from the image data and hence called as the data term. The weighting functions and apply to the smoothing and data terms, respectively and they are chosen as and $g(|\nabla f|) = \mu$ and $h(|\nabla f|) = |\nabla f|^2$. $g(\cdot)$ is constant here and smoothing occurs everywhere, while $h(\cdot)$ grows larger near strong edges and dominates at boundaries. Hence,

the GVF field is defined as the vector field v(x,y)=[u(x,y),v(x,y)] that minimizes the energy functional

$$\varepsilon = \iint \mu(u_x^2 + u_y^2 + v_x^2 + v_y^2) + |\nabla f|^2 |v - \nabla f|^2 \, dxd \qquad (8)$$

The effect of this variational formulation is that the result is made smooth when there is no data. When the gradient of the edge map is large, it keeps the external field nearly equal to the gradient, but keeps field to be slowly varying in homogeneous regions where the gradient of the edge map is small, i.e., the gradient of an edge map Δf has vectors point toward the edges, which are normal to the edges at the edges and have magnitudes only in the immediate vicinity of the edges and in homogeneous regions Δf is nearly zero. μ is a regularization parameter that governs the tradeoff between the first and the second term in the integrand in Eq. 8. The solution of Eq. 8 can be done using the Calculus of Variations and further by treating u and v as functions of time, solving them as generalized diffusion equations (Xu and Prince, 1998).

DISCRETE COSINE TRANSFORM (DCT) BASED GVF ACTIVE CONTOURS

The transform of an image yields more insight into the properties of the image. The DCT has excellent energy compaction. Hence, the DCT promises better description of the image properties.

The DCT is embedded into the GVF Active Contours. When the image property description is significantly low, this helps the contour model to give significantly better performance by utilizing the energy compaction property of the DCT.

The 2D DCT is defined as:

$$C(u,v) = \alpha(u)\alpha(v)\sum_{x=0}^{N-1}\sum_{y=0}^{N-1} f(x,y)\cos\left[\frac{(2x+1)u\pi}{2N}\right]\cos\left[\frac{(2y+1)v\pi}{2N}\right] \qquad (9)$$

The local contrast of the Image at the given pixel location (k,l) is given by:

$$P(k,l) = \frac{\sum_{t=1}^{2(2n+1)-1} w_t E_t}{d_{00}} \qquad (10)$$

Where:

$$E_t = \frac{\sum_{u+v=t} |d_{u,v}|}{N} \qquad (11)$$

and

$$N = \begin{cases} t+1 & t<2n+1 \\ 2(2n+1)-t & t\geq 2n+1 \end{cases} \qquad (12)$$

Here, w_t denotes the weights used to select the DCT coefficients. The local contrast P(k,l) is then used to generate a DCT contrast enhanced image (Tang and Acton, 2004), which is then subject to selective segmentation by the energy compact Gradient Vector Flow Active Contour Model using Eq. 8.

NGVF ACTIVE CONTOURS

NGVF is an improved external force field for Active Contour Model (Jifeng *et al.*, 2007). Based on analyzing the diffusion process of the GVF and three interpolation functions, it has been found that the generation of GVF contains diffusions in two orthogonal directions along the edge of image, one is the tangent direction and the other is the normal direction. Moreover, the diffusion in the normal direction plays the key role on the diffusion of GVF, while the diffusion in the tangent direction has little effect. So the GVF in the normal direction (NGVF) is taken as a new force field to study. Experiment results with several test images revealed that, compared with GVF, NGVF can enter into long, thin indention and had faster convergence speed towards the concavity and bigger time step (Jifeng *et al.*, 2007).

NGVF is differentiated from GVF by diffusion term and can be also considered as a special case of GVF force field. Moreover, compared with GVF, NGVF can enter into long and thin concavity. It is important that bigger time step makes NGVF more effective than GVF in some cases. In addition, the interpolation function is associated with diffusion process of force field, helping to provide some insights to construct better force fields. The formulation of the NGVF is given in Jifeng *et al.* (2007).

DCT BASED NGVF ACTIVE CONTOURS

The DCT based GVF Active Contours have been proved to yield efficient segmentation results using standard characterized parameter values for the formulation of the Active Contours. Also, the DCT based GVF Active Contours have been found to be robust, yielding accurate and efficient segmentation results under varying conditions (Britto and Ravindran, 2005a, b; 2006a-e; 2007a, b). The NGVF (Jifeng *et al.*, 2007) has faster convergence speed towards the concavity and bigger time step. It also has the capability to enter into long, thin indention and provide a good contour.

The DCT based NGVF Active Contours (Britto and Ravindran, 2007c) has the combined strengths of the DCT

based GVF Active Contour formulation (Britto and Ravindran, 2005a, b; 2006a-e; 2007a, b) and the NGVF formulation (Jifeng *et al*., 2007). The formulation for the new hybrid technique DCT based NGVF Active Contours (Britto and Ravindran, 2007c) is as follows: The local contrast term in Eq. 10 is used to generate a DCT contrast enhanced image, which is then be subject to segmentation using the NGVF Active Contours, giving rise to the formulation of the hybrid technique DCT based NGVF Active Contours.

EXPERIMENTAL RESULTS AND DISCUSSION

Britto and Ravindran (2007c) have used DCT based GVF standardized characterized parameter values directly in the DCT based NGVF Active Contour formulation without any modifications. Under strict evaluation conditions, the DCT based NGVF Active Contours yielded good segmentation results (Britto and Ravindran, 2007c).

In this study, the merit of the DCT based NGVF Active Contours is evaluated by experimentally comparing with the DCT based GVF Active Contours. DCT based GVF Active Contours have already been established to be an efficient segmentation technique for chromosome images (Britto and Ravindran, 2005a, b; 2006a-e; 2007a, b). Using DCT based GVF Active Contours as benchmark for evaluation, DCT based NGVF Active Contours have been evaluated comparatively for chromosome image segmentation.

Experiments were performed under the strict evaluation conditions outlined in Britto and Ravindran (2007c) on both DCT based NGVF Active Contours and DCT based GVF Active Contours. On Plate 1, forty sample images were used for this experimentation. Samples 1-40 show the original sample images. Samples 41-80 show the DCT based GVF Active Contour segmented images. Samples 81-120 show DCT based NGVF Active Contour segmented images. The Graphical results show that both the techniques, namely the DCT based NGVF Active Contours and the DCT based GVF Active Contours yielded very good segmentation results. Visual inspection of DCT based GVF Active Contour segmented chromosome images and DCT based NGVF Active Contour images show that segmentation has been successful. All 40 samples segmented using both the techniques have been displayed here to indicate that both the techniques show similar segmentation performance visually. Therefore quantitative comparative evaluation was done to judge the better of the two techniques *viz*., DCT based GVF Active Contours and DCT based NGVF Active Contours.

Quantitative Evaluation of the DCT based NGVF Active Contour compared with the DCT based GVF Active Contour segmentation has been done and shown in Table 1. The mean of the respective errors along the corresponding axes of the contours obtained on segmentation using DCT based NGVF Active Contours and DCT based GVF Active Contours show a variation of approximately 0.1 pixels. Compared with the 1 pixel contour step size and the 1 pixel width of the contour, a variation of 0.1 pixels may be insignificant. Hence the variation of approximately 0.1 pixels is negligible.

But the percentage variation of the ratio of the major axis error of the contour to the minor axis error of the contour show a significant reduction of -6.46% in DCT based NGVF Active Contours compared to DCT based GVF Active Contours. This implies that the DCT based NGVF Active Contours are more symmetric compared to the DCT based GVF Active Contours and the error is more uniform along the major and minor axes, implying that eccentric errors in the DCT based GVF Active Contours are reduced in the DCT based NGVF Active Contours.

Percentage variation of the ratio of the contour major axis radius to the minor axis radius of the DCT based NGVF Active Contours compared with the DCT based GVF Active Contours shows a reduction of -0.84%. This supports the earlier inference that the DCT based NGVF Active Contours are more symmetric compared with the DCT based GVF Active Contours. It had been established that the DCT based GVF Active Contours are an efficient segmentation technique for chromosome images (Britto and Ravindran, 2005a, b, 2006a-e, 2007a, b). The symmetric behavior of the DCT based NGVF Active Contour promises scope for better and improved segmentation compared with the DCT based GVF Active Contour.

Reduction in segmentation errors indicate better approximation of the original boundary by the Active Contour segmented boundary. Reduction in ratios of errors (Table 1) indicate symmetricity of the Active Contour, which infers that the Active Contour boundary is independent of the typical shape (axial elongation) of the chromosome. These inferences point in the direction of the DCT based NGVF Active Contours as a more efficient segmentation technique.

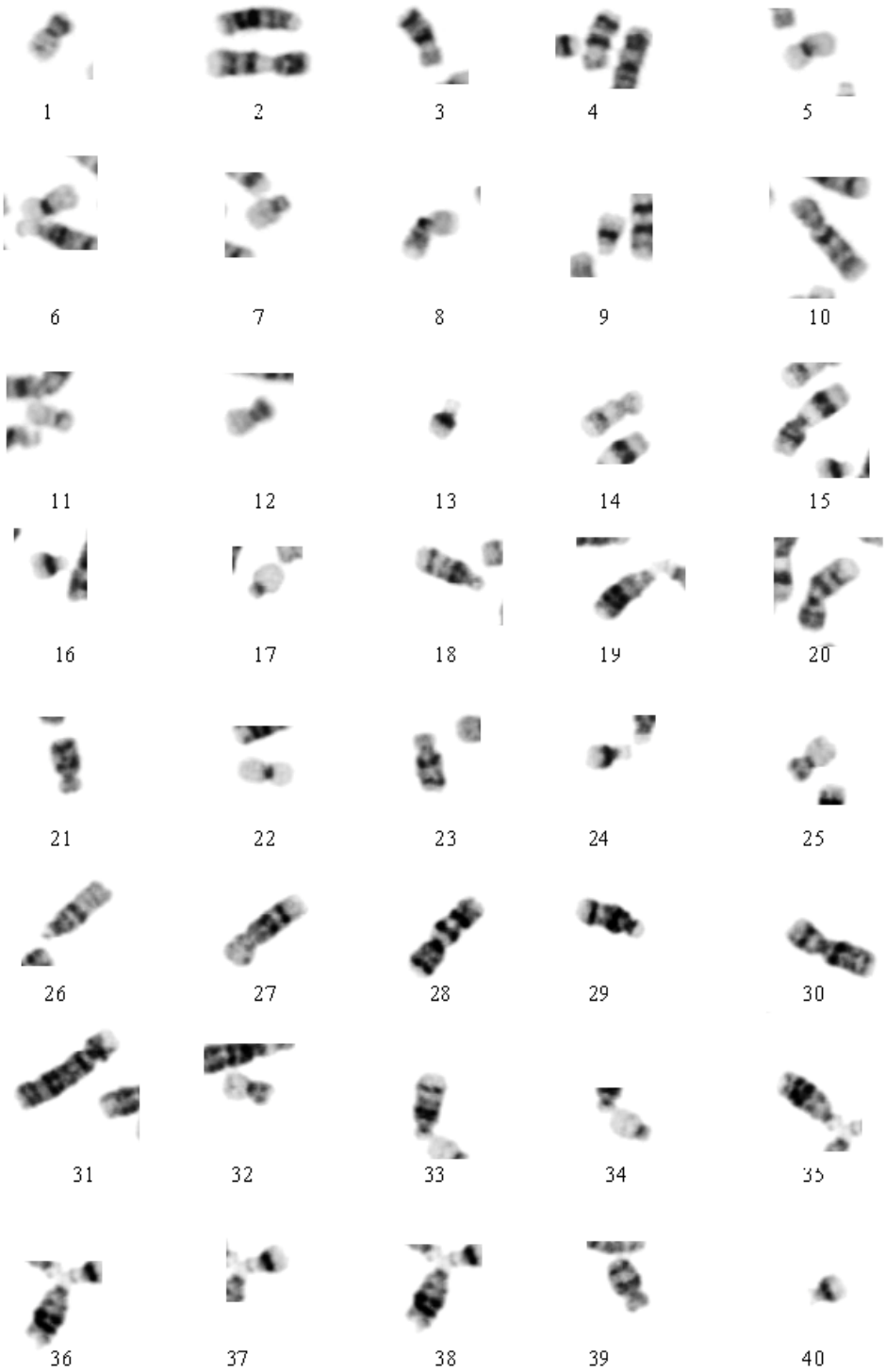

Plate 1: Samples 1 to 40 show the original sample image without the DCT based GVF and DCI based NGVF. Active Contour segmented images. The original sample images in gray color

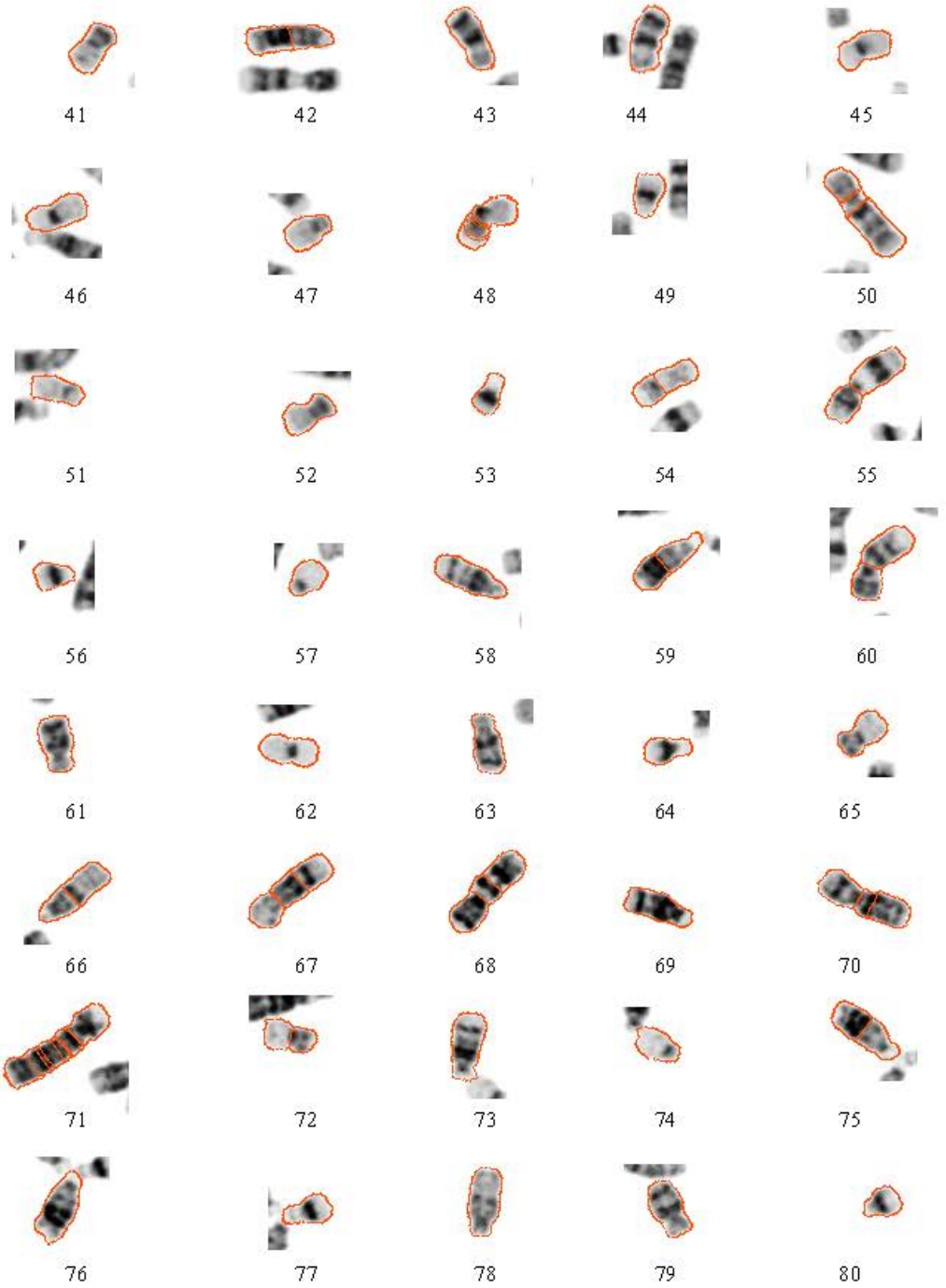

Plate 1: Samples 41 to 80 show the corresponding DCT based GVF Active Contour segmented images with the mapped boundary indicated in red color. Visual inspection of DCT based GVF Active Contour segmented chromosome images and DCT based NGVF active contour images show that segmentation has been successful. All 40 samples segmented using both the techniques have been displayed here to indicate that both the techniques show similar segmentation performance visually

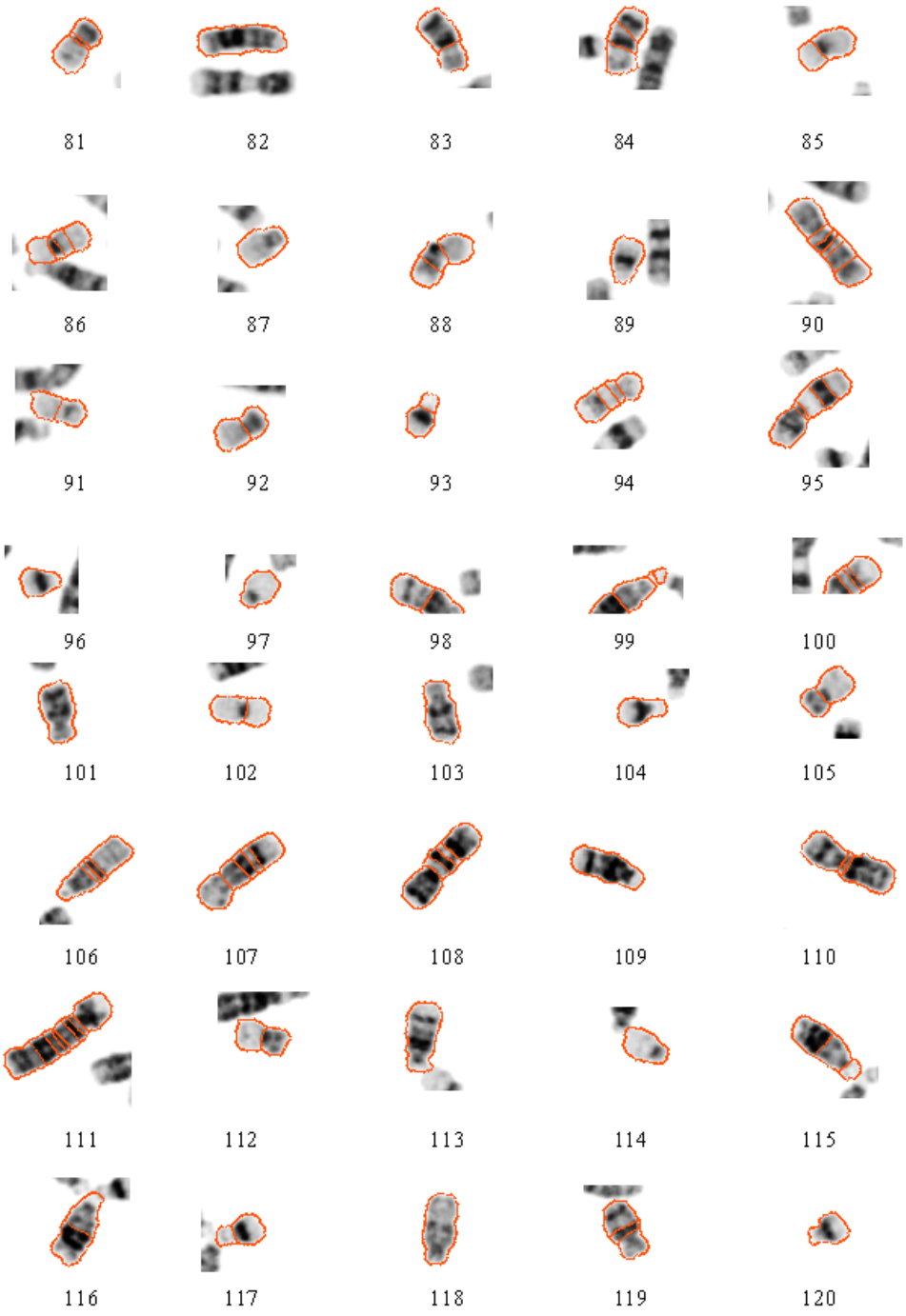

Plate 1: Samples 81 to 120 show the corresponding DCT based NGVF Active Contour segmented images with the mapped boundary indicated in red color. Visual inspection of DCT based GVF active contour segmented chromosome images and DCT based NGVF active contour images show that segmentation has been successful. All 40 samples segmented using both the techniques have been displayed here to indicate that both the techniques show similar segmentation performance visually

Table 1: Quantitative Comparative Evaluation of the DCT based NGVF Active Contours against DCT based GVF Active Contours based on the contour segmentation errors and their ratios

	GVFDCT					NGVFDCT				
Sample No.	Major axis radial error (original -contour) (pixels)	Minor axis radial error (original -contour) (pixels)	Ratio of major axis error to minor axis error	Ratio of original image major axis radius to minor axis radius	Ratio of contour major axis radius to minor axis radius	Major axis radial error (original -contour) (pixels)	Minor axis radial error (original -contour) (pixels)	Ratio of major axis error to minor axis error	Ratio of original image major axis radius to minor axis radius	Ratio of contour major axis radius to minor axis radius
1	-1.44	-1.86	0.78	1.80	1.66	-1.52	-1.77	0.86	1.79	1.66
2	-1.95	-1.11	1.77	3.21	3.07	-1.89	-1.38	1.37	3.05	2.86
3	-1.16	-1.66	0.69	2.34	2.11	-1.20	-1.55	0.77	2.12	1.96
4	-1.39	-1.56	0.89	2.08	1.93	-1.48	-1.62	0.92	2.03	1.89
5	-1.49	-1.68	0.89	1.92	1.78	-1.42	-1.85	0.77	1.97	1.79
6	-1.45	-1.63	0.89	2.20	2.02	-1.75	-1.89	0.92	2.31	2.09
7	-1.45	-1.77	0.82	1.60	1.49	-1.61	-1.93	0.84	1.59	1.48
8	-1.83	-1.54	1.19	2.11	2.00	-1.90	-1.48	1.29	2.07	1.98
9	-1.37	-1.68	0.82	1.55	1.45	-1.40	-1.82	0.77	1.54	1.43
10	-1.56	-1.81	0.86	3.46	3.10	-1.57	-1.68	0.94	3.52	3.19
11	-1.39	-1.71	0.82	2.27	2.03	-1.54	-1.91	0.81	2.21	1.97
12	-1.44	-1.83	0.79	1.95	1.77	-1.64	-1.65	0.99	1.83	1.72
13	-1.95	-1.32	1.48	1.65	1.62	-1.82	-1.54	1.18	1.73	1.65
14	-1.67	-1.79	0.93	2.71	2.42	-1.93	-1.90	1.02	2.56	2.31
15	-1.47	-1.58	0.93	3.28	2.98	-1.57	-1.64	0.96	3.27	2.97
16	-1.86	-1.30	1.43	1.52	1.51	-1.83	-1.15	1.59	1.43	1.44
17	-1.49	-1.75	0.85	1.39	1.31	-1.46	-1.80	0.81	1.37	1.29
18	-1.78	-1.50	1.19	2.70	2.50	-1.86	-1.73	1.07	2.70	2.47
19	-1.97	-1.27	1.55	2.78	2.65	-1.80	-1.57	1.15	3.03	2.78
20	-1.17	-1.57	0.74	2.51	2.31	-0.30	-1.67	0.18	2.49	2.22
21	-1.22	-1.64	0.75	1.79	1.66	-1.49	-1.80	0.83	1.83	1.70
22	-1.75	-2.00	0.88	2.16	1.94	-1.79	-1.76	1.02	2.20	2.02
23	-1.54	-1.31	1.17	2.13	2.02	-1.37	-1.67	0.82	2.05	1.89
24	-1.91	-1.34	1.43	1.92	1.85	-1.91	-1.45	1.32	1.91	1.83
25	-0.93	-1.69	0.55	1.83	1.65	-1.48	-1.85	0.80	1.88	1.72
26	-1.31	-1.70	0.77	2.89	2.59	-1.90	-1.68	1.13	2.92	2.67
27	-1.44	-1.66	0.86	3.28	2.97	-1.55	-1.79	0.87	3.25	2.93
28	-1.38	-1.37	1.01	3.20	2.97	-1.62	-1.49	1.09	3.20	2.96
29	-2.38	-0.68	3.52	2.41	2.48	-2.20	-1.13	1.94	2.52	2.47
30	-1.71	-1.26	1.36	3.20	3.01	-1.75	-1.45	1.21	3.16	2.94
31	-1.63	-1.34	1.22	3.92	3.64	-1.62	-1.53	1.06	3.92	3.58
32	-1.37	-1.40	0.98	1.89	1.78	-1.44	-1.61	0.90	1.85	1.72
33	-1.62	-1.47	1.10	2.18	2.06	-1.90	-1.57	1.21	2.18	2.07
34	-1.44	-1.89	0.76	1.68	1.53	-1.78	-1.88	0.95	1.65	1.54
35	-1.91	-1.50	1.28	2.52	2.37	-2.05	-1.57	1.30	2.65	2.48
36	-2.03	-1.31	1.54	2.21	2.15	-2.05	-1.55	1.32	2.25	2.14
37	-1.74	-1.34	1.29	1.88	1.81	-1.53	-1.80	0.85	1.81	1.66
38	-1.35	-1.54	0.88	2.20	2.04	-1.38	-1.73	0.80	2.21	2.02
39	-1.18	-1.28	0.92	1.84	1.75	-1.40	-1.51	0.93	1.83	1.73
40	-1.53	-1.58	0.97	1.33	1.28	-1.82	-1.53	1.18	1.38	1.35
Mean	-1.57	-1.53	1.09	2.29	2.13	-1.64	-1.65	1.02	2.28	2.11
						% Variation with GVFDCT		-6.46		-0.84

Table 1 shows the quantitative evaluation of the merit of the DCT based NGVF Active Contours against DCT based GVF Active Contours based on the contour segmentation errors and their ratios. Reduction in segmentation errors indicate better approximation of the original boundary by the Active Contour segmented boundary. Reduction in ratios of errors (shown in Table above) indicate symmetricity of the Active Contour, which infers that the Active Contour boundary is independent of the typical shape (axial elongation) of the chromosome

CONCLUSION

This research work establishes that the DCT based NGVF Active Contours show almost similar error measures compared to the DCT based GVF Active Contours. This implies that the DCT based NGVF Active Contours should be as good and efficient as the DCT based GVF Active Contours. One special behavior of the DCT based NGVF Active Contour has also been observed and reported in this study. The DCT based NGVF Active Contours are more symmetric compared to the DCT based GVF Active Contours. This symmetric behavior of the DCT based NGVF Active Contours promises improved and better segmentation performance. Compared with DCT based GVF Active Contours, these inferences point in the direction of the DCT based NGVF Active Contours as a more efficient segmentation technique.

ACKNOWLEDGMENTS

The authors express their thanks to Dr. Michael Difilippantonio (Staff Scientist at the Section of Cancer Genomics, Genetics Branch/CCR/NCI/NIH, Bethesda MD); Prof. Ekaterina Detcheva (Artificial Intelligence Department, Institute of Mathematics and Informatics, Sofia, Bulgaria); Prof. Ken Castleman and Prof. Qiang Wu (Advanced Digital Imaging Research, Texas); Wisconsin State Laboratory of Hygiene (http://worms.zoology.wisc.edu/zooweb/Phelps/karyotype.html) and the Genomic Centre for Cancer Research and Diagnosis (GCCRD) (http://www.umanitoba.ca/institutes/manitoba_institute_cell_biology/GCCRD/GCCRD_Homepage.htm) for providing chromosome spread images. The authors thank Prof. Ning Jifeng, Xidian University, Shaanxi, China.

REFERENCES

Britto, A.P. and G. Ravindran, 2005a. A review of deformable curves from the perspective of chromosome image segmentation. J. Med. Sci., 5 (4): 363-370.

Britto, A.P. and G. Ravindran, 2005b. Comparison of boundary mapping efficiency of Gradient Vector Flow Active Contours and their variants on chromosome spread images. J. Applied Sci., 5 (8): 1452-1460.

Britto, A.P. and G. Ravindran, 2006a. Boundary mapping of chromosome spread images using optimal set of parameter values in Discrete Cosine Transform Based Gradient Vector Flow Active Contours. J. Applied Sci., 6 (6): 1351-1361.

Britto, A.P. and G. Ravindran, 2006b. Detection of specific human chromosomal abnormalities using Discrete Cosine Transform Based Gradient Vector Flow Active Contours. Biotechnology, 5 (1): 111-117.

Britto, A.P. and G. Ravindran, 2006c. Evaluation of standardization of curve evolution based boundary mapping technique for chromosome spread images. Inform. Technol. J., 5 (1): 94-107.

Britto, A.P. and G. Ravindran, 2006d. Segmentation of chromosome spread images using Discrete Cosine Transform Based Gradient Vector Flow Active Contours, an analysis. J. Med. Sci., 6 (1): 117-124.

Britto, A.P. and G. Ravindran, 2006e. Evaluation of Discrete Cosine Transform Based Gradient Vector Flow Active Contours as an efficient tool for boundary mapping of chromosome spread images. Acad. Open Internet J., www.acadjournal.com/2006/v19/part1/p1/EvaluationDCT.pdf.

Britto, A.P. and G. Ravindran, 2007a. Novel findings in chromosome image segmentation using Discrete Cosine Transform Based Gradient Vector Flow Active Contours. Inform. Technol. J., 6 (1): 1-7.

Britto, A.P. and G. Ravindran, 2007b. Review of deformable curves-A retro analysis. Inform. Technol. J., 6 (1): 26-36.

Britto, A.P. and G. Ravindran, 2007c. Discrete Cosine Transform Based Gradient Vector Flow in normal direction Active contours. Inform. Technol. J., 6 (7): 1050-1056.

Jifeng, N., W. Chengke, L. Shigang and Y. Shuqin, 2007. NGVF: An improved external force field for Active Contour Model. Patt. Recog. Lett., 28 (1): 58-63.

Kass, M., A. Witkin and D. Terzopoulos, 1987. Snakes: Active Contour Models. Int. J. Comp. Vision, 1 (4): 321-331.

Prince, J.L. and C. Xu, 1996. A new external force model for snakes. In 1996 Image and Multidimensional Signal Processing Workshop, pp: 30-31.

Rueckert, D., 1997. Segmentation and tracking in cardiovascular MR images using geometrically deformable models and templates. Ph.D Thesis, Imperial College of Science, Technology and Medicine, London.

Tang, J. and S.T. Acton, 2004. A DCT based Gradient Vector Flow snake for object boundary detection. Image Analysis and Interpretation. 6th IEEE Southwest Symposium, pp: 157-161.

Xu, C. and J.L. Prince, 1997. Gradient Vector Flow: A new external force for snakes. IEEE Proc. Conf. on Comp. Vis. Patt. Recog. (CVPR) pp: 66-71.

Xu, C. and J.L. Prince, 1998. Snakes, shapes and Gradient Vector Flow, IEEE Trans. Image Proc., 7 (3): 359-369.

Xu, C. and J.L. Prince, 2000. Gradient Vector Flow Deformable Models. In: Handbook of Medical Imaging, Academic Press, pp: 159-170.